



HAL
open science

Hypervelocity impact into a high strength and ductile steel alloy

E. Lach, C. Anderson, V. Schirm, G. Koerber

► **To cite this version:**

E. Lach, C. Anderson, V. Schirm, G. Koerber. Hypervelocity impact into a high strength and ductile steel alloy. *International Journal of Impact Engineering*, 2008, 35 (12), pp.1625. 10.1016/j.ijimpeng.2008.07.008 . hal-00542560

HAL Id: hal-00542560

<https://hal.science/hal-00542560>

Submitted on 3 Dec 2010

HAL is a multi-disciplinary open access archive for the deposit and dissemination of scientific research documents, whether they are published or not. The documents may come from teaching and research institutions in France or abroad, or from public or private research centers.

L'archive ouverte pluridisciplinaire **HAL**, est destinée au dépôt et à la diffusion de documents scientifiques de niveau recherche, publiés ou non, émanant des établissements d'enseignement et de recherche français ou étrangers, des laboratoires publics ou privés.

Accepted Manuscript

Title: Hypervelocity impact into a high strength and ductile steel alloy

Authors: E. Lach, C. Anderson, V. Schirm, G. Koerber



PII: S0734-743X(08)00144-9

DOI: [10.1016/j.ijimpeng.2008.07.008](https://doi.org/10.1016/j.ijimpeng.2008.07.008)

Reference: IE 1626

To appear in: *International Journal of Impact Engineering*

Received Date:

Revised Date:

Accepted Date:

Please cite this article as: Lach E, Anderson C, Schirm V, Koerber G. Hypervelocity impact into a high strength and ductile steel alloy, *International Journal of Impact Engineering* (2008), doi: [10.1016/j.ijimpeng.2008.07.008](https://doi.org/10.1016/j.ijimpeng.2008.07.008)

This is a PDF file of an unedited manuscript that has been accepted for publication. As a service to our customers we are providing this early version of the manuscript. The manuscript will undergo copyediting, typesetting, and review of the resulting proof before it is published in its final form. Please note that during the production process errors may be discovered which could affect the content, and all legal disclaimers that apply to the journal pertain.

Hypervelocity impact into a high strength and ductile steel alloy

E. Lach^{* a)}, C. Anderson^{b)}, V. Schirm^{a)}, G. Koerber^{a)}

^{a)} French-German Research Institute of Saint-Louis, P.O. Box 70034, 68301 Saint-Louis, France

^{b)} Southwest Research Institute, 6220 Culebra Road, San Antonio, TX 78228-0510, USA

Abstract

The unusual properties of nitrogen alloyed austenitic steels have been reported in the recent two decades in many papers. In this work it is aimed to investigate a P900 alloy subjected to a hypervelocity impact. The P900 alloy was work hardened to a medium hardness of 380 HV30 by cold expansion of a ring. Tungsten heavy metal and pure tungsten were used as projectile materials. The geometry of the long rods was 3 mm · 30 mm for diameter and length, respectively. Ballistic tests were performed with a two stage light-gas gun at velocities from about 2000 m/s up to about 4500 m/s. It was found that two kinds of crater geometry are possible depending on the tendency of the projectile material to adiabatic shear banding or brittle fracture. The brittle W material achieved a deeper crater than the shear band forming W heavy alloy.

Keywords: Hypervelocity impact; Nitrogen alloyed austenitic steels; Pure tungsten; Tungsten heavy alloy

1. Introduction

In reference [1] it was shown that nitrogen alloyed austenitic steels have under dynamic loading a performance, which is considerably increased compared to the quasi-static properties. The ballistic protection capability was compared and found to be similar to that of a conventional armor steel at an impact velocity of 2500 m/s. Quasi-static and dynamic compression tests performed on P900 and conventional armor steel confirmed this result. Hardness measurements revealed an increased hardness around the crater of nitrogen alloyed steels, whilst the hardness of conventional armor steels did not change. In this work it is aimed to investigate the ballistic protective capability of nitrogen alloyed austenitic steels under high velocity impact ranging from about 2000 m/s up to about 4500 m/s.

Nitrogen alloyed austenitic steels are interstitially alloyed with a considerable amount of nitrogen. It is a relatively new group of material, which is still in development. Nitrogen has to be in solid solution and then it is resulting in unusual combinations of strength, toughness, corrosion resistance, wear resistance and non-magnetizability [2]. The solubility of nitrogen is increased by Cr, Mn, Mo and V and decreased by Ni and Si. [3, 4]. Nitrogen in solid solution prevents the formation of deformation

* Corresponding author. Tel.: +33 389 69 50 88; fax: +33 389 69 53 59.

E-mail address: lach@isl.tn.fr

martensite α' and enables a materials deformation of more than 95 % without austenite becoming instable. It also leads to a plane arrangement of dislocations and the very low stacking fault energy due to the nitrogen content shifting the onset of mechanical twinning to lower strain. This micro mechanism extends strongly the plastic deformation capability, because the macroscopic plastic deformation related to dislocation gliding is limited. In reference [5] it is described how nitrogen alloyed steels may achieve the very high tensile strength of 3380 MPa due to work hardening and a thermal treatment.

The nitrogen alloyed austenitic steels are interesting because of their extraordinary mechanical properties. Nitrogen in solution increases not only the strength and ductility, but also strongly the internal friction resulting in enormously high strain rate sensitivity. These properties make nitrogen alloyed austenitic steels a potential candidate as an armor material, but which now must be studied under the conditions of ballistic impact/penetration.

2. Experimental Setups

Quasi-static compression and tensile tests have been performed at room temperature on a universal test machine at strain rates of about $5 \cdot 10^{-3} \text{ s}^{-1}$. Dynamic compression and tensile tests at strain rates ranging from $1 \cdot 10^3 \text{ s}^{-1}$ to $5 \cdot 10^3 \text{ s}^{-1}$ were conducted at room temperature using a split-Hopkinson-pressure-bar (SHPB) and a Hopkinson tensile bar. Compression tests specimens (5 mm in diameter and 4 to 5 mm in length) were cut from the P900 material using electro-discharge machining. Tensile specimens were turned on a lathe. Subsequently, the specimens were ground to obtain smooth surfaces. Prior to testing the compression test specimens were lubricated with ball bearing grease in order to reduce frictional effects.

Ballistic tests were performed with a two stage light-gas gun at velocities ranging from about 2000 m/s up to 4500 m/s. The launch tube is 6 m long and has a caliber diameter of 30 mm. In the hyperballistic tunnel there was a pressure of 420 Torr. The geometry of the rods was 3 mm in diameter and 30 mm in length ($L/D = 10$). To determine hardness the Vickers test was used. It can be defined as indentation hardness testing that involves forcing a diamond indenter of square-based pyramidal geometry with face angles of 136° into the surface of the test material. Parameters used for the macroscopic hardness tests are a mass of 30 kg and a duration of 30 seconds.

3. Materials Behavior

3.1 Long rod material

Rods consist of a tungsten heavy metal (W=94%, density= 17.85 g/cm^3), which tends to create adiabatic shear bands (ASB). For comparison to rods showing brittle behavior pure tungsten was used. The dynamic true stress-strain compression curves of the rod materials are shown in Fig. 1. Pure W possesses a compression strength of 2000 MPa, while W heavy metal exceeds slightly the compression strength of 2000 MPa. W heavy metal fractures due to ASB, while pure W fractures brittle.

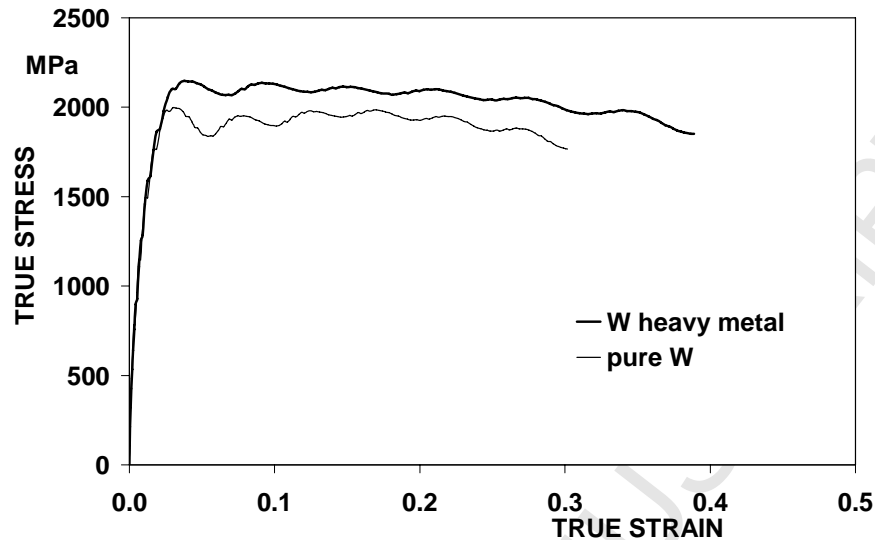


Fig. 1. Dynamic true stress-strain compression curves of the rod materials

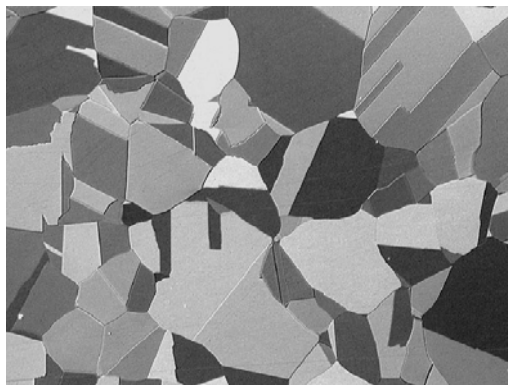
3.2 Target material

A nitrogen alloyed austenitic steel designated X8 Cr Mn N 18 18 (ASTM A289, DIN-Code 1.3816) was employed for the targets. This alloy is well known as P900. The chemical composition of the investigated nitrogen alloyed steel is shown in Table 1. The steel alloy was supplied in cold worked condition (cold expansion) up to a macro hardness of 380 HV30 in average. Some specimens from this alloy were solution annealed. In the solution annealed condition the average Vickers hardness amounts about 280 HV30. Some of the solution annealed specimens have been cold rolled to macro hardness exceeding 400 HV30 strongly and a few were subjected to a strain aging at 500°C for 10 min in order to increase further the strength.

Table 1. Chemical composition of the investigated steel (weight %)

P900	<i>C</i>	<i>Si</i>	<i>Mn</i>	<i>Cr</i>	<i>N</i>
	0.033	0.3	19.02	18.4	0.62

The microstructure of the P900 in the solution annealed status can be seen in Fig. 2(a). Figure 2(b) shows the microstructure in the supplied cold expanded status. It is characterized by slightly deformed grains and a high density of glide bands. Figure 3 summarizes the quasi-static tensile tests for different treated P900. The tensile specimen in the solution annealed condition possesses a macro hardness of 251 HV30. It has a long uniform strain about 40 % and strain hardens from 600 MPa to about 1300 MPa. Work hardening is increasing the yield stress strongly, but reduces the uniform strain and the strain hardening. The onset of striction is shifted to lower strains. The stress-strain curves obtained by dynamic tensile tests are shown in Fig. 4. By increasing the strain rate the yield strength is significantly augmented. The results obtained from quasi-static compression tests on P900 are shown in Fig. 5. The compression yield strength is strongly increased by cold working.



(a) solution annealed status



(b) cold worked (cold expanded), grains showing glide bands

Fig. 2. Microstructure of nitrogen alloyed steels

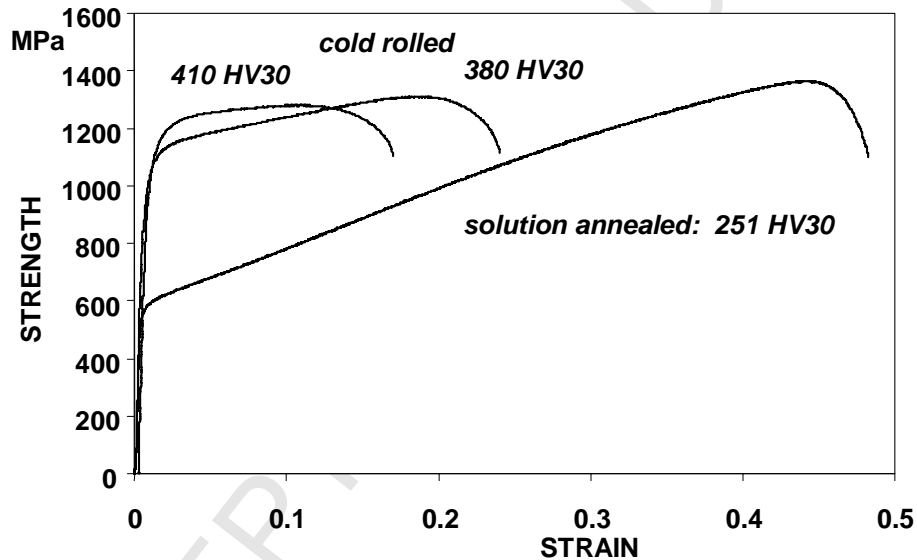


Fig. 3. Quasistatic tensile stress-strain curves for P900 obtained after various thermomechanical treatment

An additional strain aging of strongly cold worked samples increases the compression yield strength further by pinning of dislocations. Hence, this mechanism which only works effectively after a severe deformation, is a powerful way of increasing the compressive strength. Since none of the specimens was fractured during quasi-static compression, there is sufficient deformability up to a hardness of 510 HV30 under quasi-static conditions. Figure 5 also shows that strain hardening decreases with increasing cold working. Figure 6 summarizes the results of dynamic compression tests with alloy P900. It is obvious that the dynamic compressive yield stress is considerably higher than the corresponding quasi-static yield stress.

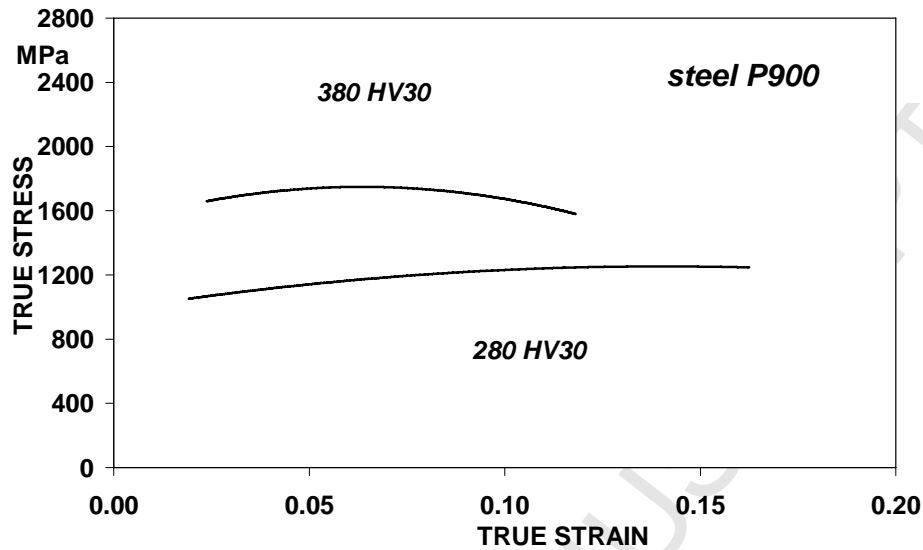


Fig. 4. Dynamic tensile stress-strain curves for P900 obtained for the solution annealed and the cold work status

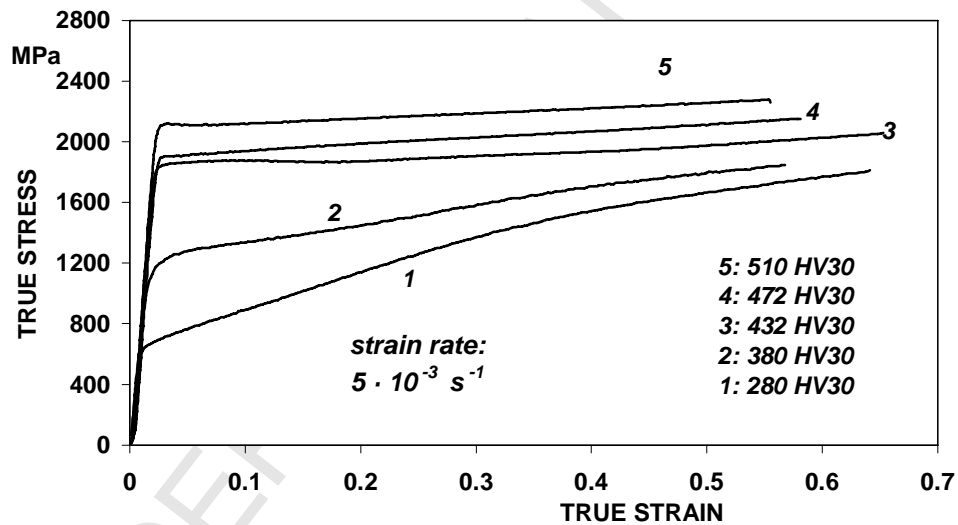


Fig. 5. Stress-strain curves for P900 obtained from quasi-static compression tests after various thermomechanical treatment

Since nitrogen in solid solution increases the internal friction of the lattice [4], the strain rate sensitivity increases. The dynamic compression yield stress of the solution annealed specimens is twice that of the corresponding quasi-static compression yield stress [6, 7]. This difference seems to decrease with increasing work hardening. In specimens with the hardness of 432 HV30 and above, adiabatic shear banding occurs in the dynamic compression test specimens resulting in a catastrophic failure.

4. Ballistic Results

For the ballistic tests semi infinite targets consisting of the P900 alloy in the cold worked status with an average hardness of 380 HV30 were applied. Figure 7 compiles the results of the ballistic tests as P/L vs projectile velocity. It shows clearly that the rod consisting of pure W has a better performance than W heavy metal up to a velocity exceeding 4000 m/s, where the difference disappears.

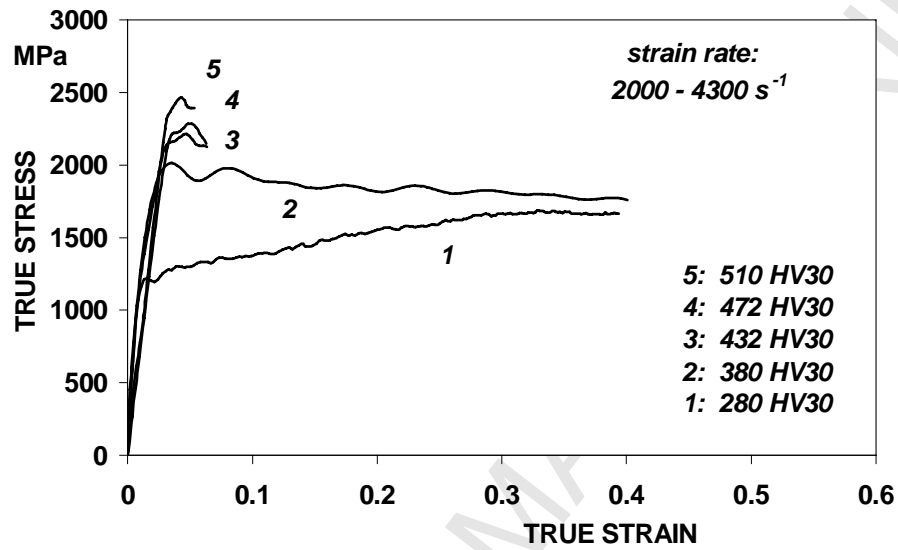


Fig. 6. Dynamic compression tests for P900 after various thermomechanical treatment

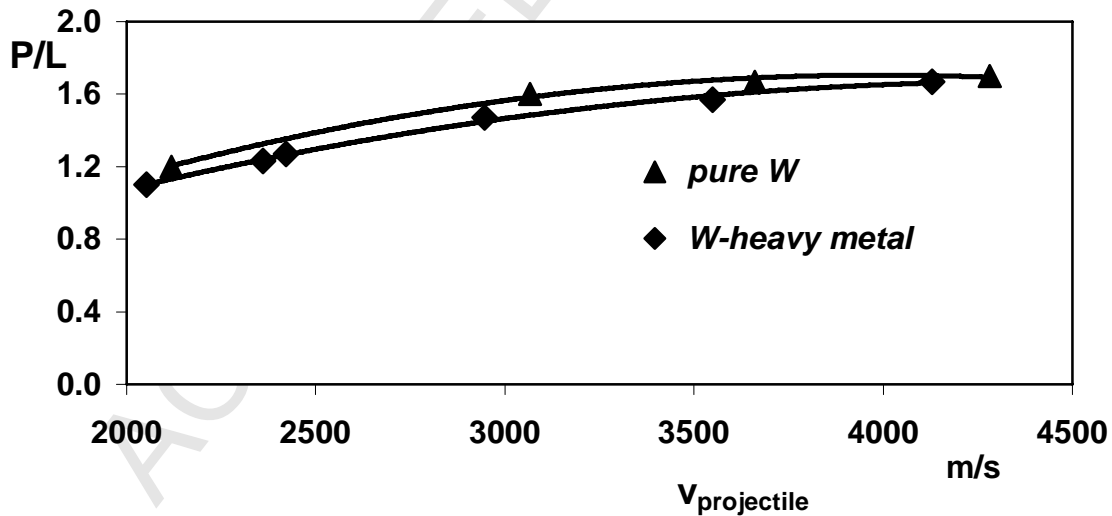
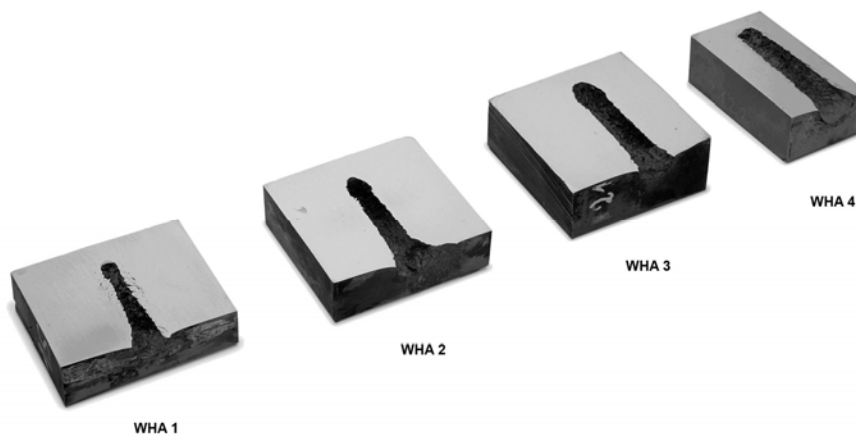


Fig. 7. Results of terminal ballistic tests, Penetration/Length vs impact velocity

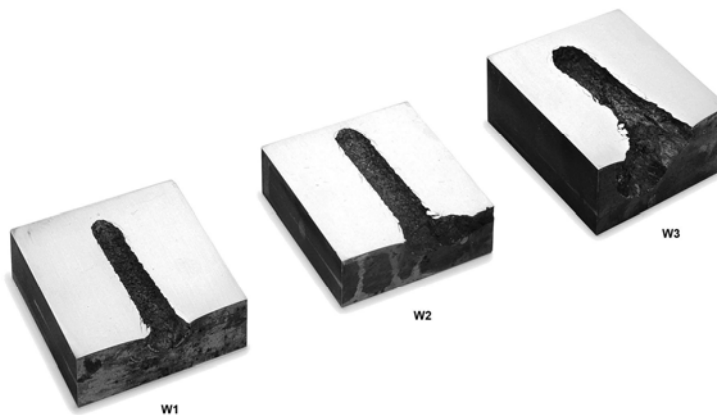
The W heavy alloy creates arrow shaped crater as it can be seen in Fig. 8. This kind of crater shaping disappears for rod velocities above 4000 m/s (WHA4 in Fig. 8).



WHA1: 2118 m/s, WHA2: 3066 m/s, WHA3: 3661 m/s, WH4: 4281 m/s

Fig. 8. Shape of the crater due to W heavy alloy rods at different impact velocities

Long rods consisting of pure W do not create craters with this shape in a similar range of impact velocity (Fig. 9).



W1: 2947 m/s, W2: 3548 m/s, W3: 4130 m/s

Fig. 9. Shape of the crater due to pure W rods at different impact velocities

5. Hardness Measurements

Two targets subjected to about a similar impact velocity but different rod material have been chosen for hardness measurements at the end of a crater. Figure 10(a) shows a crater from a W heavy

metal at a rod velocity of 3066 m/s. Along these lines the hardness measurements were performed. Figure 10(b) represents the results of the Vickers hardness measurements along the lines. The capital letters indicate the corresponding lines in Fig. 10(a).

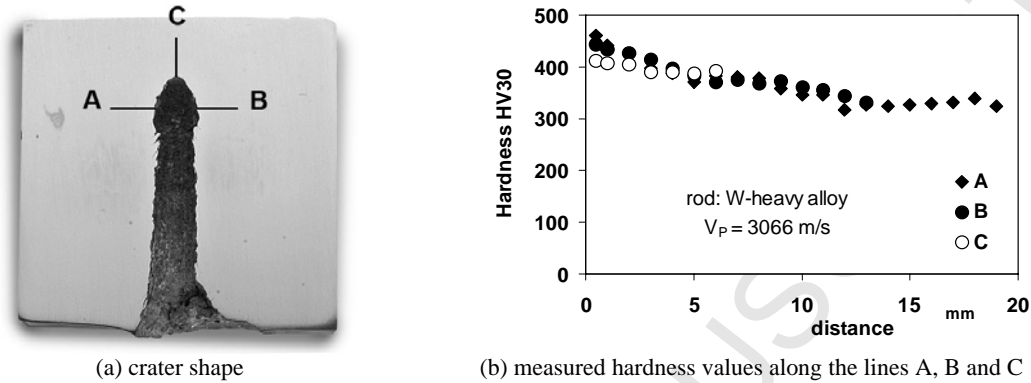


Fig. 10. Hardness measurements near the crater due to a W heavy alloy rod impact

The results in Fig. 10(b) are showing clearly that the hardness is significantly increased near the crater. This result confirms the findings, which are described in reference [1]. For the arrow shaped crater due to a rod consisting of W heavy metal the hardness at the crater tip (line C) is smaller than on both sides. The dynamic loading at the two sides of the crater must have been higher than at the tip. Figures 11(a,b) are showing the results of hardness measurements of a crater due a rod consisting of pure W. The impact velocity amounts to 2947 m/s and is close to that of figure 10. The lines in Fig. 11(a) indicate also where the hardness was measured and the capital letter the correspondence to the results in Fig. 11(b).

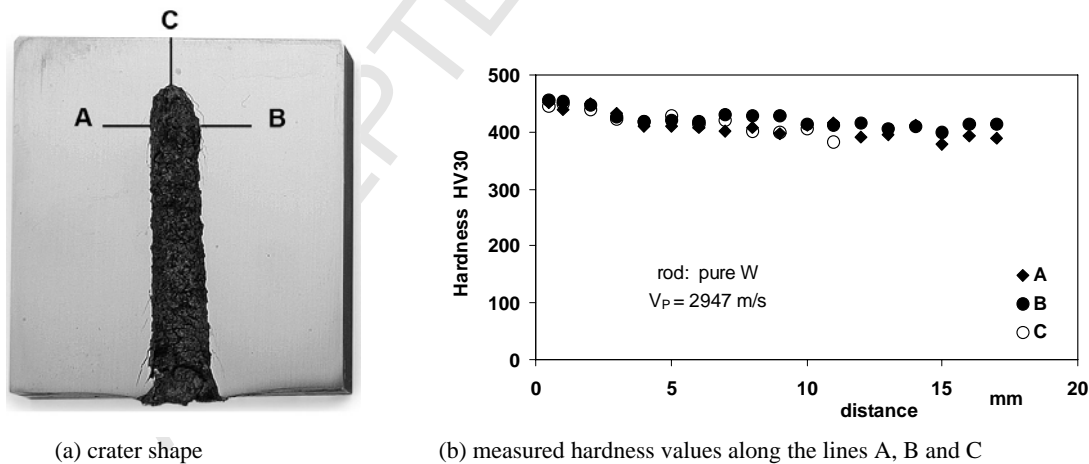


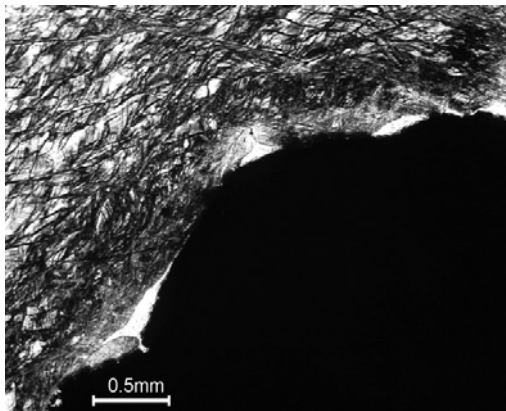
Fig. 11. Hardness measurements near the crater due to a pure W rod impact

The hardness of the target material close to the crater is also increased compared to regions of the unloaded material. Figure 11 b) shows clearly that the hardness is very similar at the crater tip and its both sides. The loading on this kind of crater end is homogeneous.

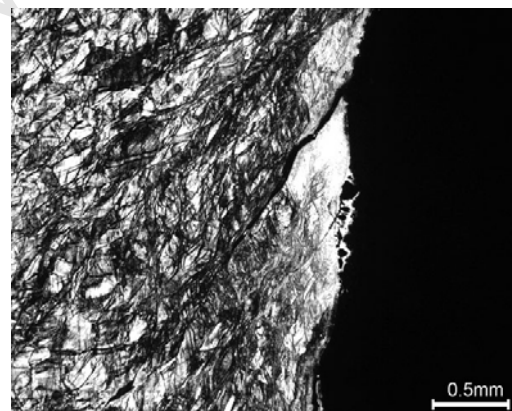
6. Microstructure

The two crater shown in Figs. 10 and 11 were subjected to a metallographic investigation. Figure 12(a) shows the tip of the arrow shaped crater of Fig. 10. The microstructure close to the crater tip is characterized by a high density of glide bands, which indicate a severe deformation. Some traces of W at the inside of the crater are also to notice. It is obviously that no micro cracking due to the formation of ASB occurred. A micrograph from the left side of the crater is shown in Fig. 12(b). The microstructure was also objected to a severe plastic deformation as the high density of glide bands and the strongly deformed grains show. Additionally the microstructure shows a crack. This crack reveals that adiabatic shear banding occurred and the plastic deformation was higher compared to the crater tip.

The micrograph in Figs. 13(a,b) shows the microstructure of the crater from Fig. 11. Figure 13(a) gives an overview about the microstructure at the crater tip. The grains are severely plastically deformed with a high density of glide bands inside. A high density of micro cracks is becoming evident and reveals that this region was objected to a strong plastic deformation. Figure 13(b) shows details of Fig. 13(a). At the crater wall traces of W from the rod are visible. The target material is a white etching phase around the tip of the crater. All this details of the microstructure refer to a strongly plastically deformed zone. At the left and right side of the crater no formation of micro cracks could be found.

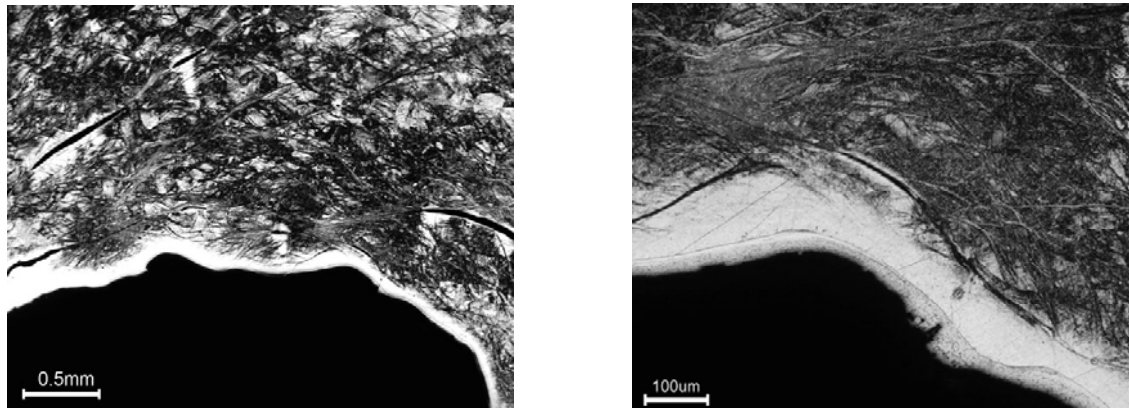


(a) no micro cracking at the tip, but a high density of glide bands in the strongly deformed grains



(b) micro cracks at the side near the tip of the crater

Fig. 12. Microstructure of the crater from figure 10



(a) a high density of micro cracks in the region of the crater tip and a white etching layer at the edge

(b) detail of the crater tip, a continuous layer of W on a white etching layer of the target alloy

Fig. 13. Microstructure of the crater from Fig. 11

7. Conclusions

Nitrogen alloyed austenitic steels are strongly strain rate sensitive as quasi-static and dynamic tensile and compression tests showed. A work hardening process increases the yield strength strongly. Compression tests have shown that under dynamic loading a too strong work hardening leads to a brittle behavior. An optimal hardness has to be discovered for nitrogen alloyed steels subjected to dynamic loading. The first few percent of dynamic plastic deformation is transient where the work hardening coefficient is extremely high. So the material strain hardens very fast under dynamic impacts. Only dynamic loadings reveal the potential of these alloys. All hardness measurements have shown that only at a narrow zone around the crater the hardness is significantly increased compared to the initial hardness. The rods consisting of W heavy metal form ASBs due to adiabatic heating. At the last stage of the long rod penetration the rod material is strongly softened by adiabatic heating and adiabatic shear banding occurs. The target material in front of the rod is strongly strain hardened and resists a further penetration. This is the reason why the ASB creating material penetrates into the both sides of the crater and creates an arrow shaped crater. The temperature of the pure W is also increased, but the material keeps its brittle behavior. Therefore the penetration process continues to deeper craters. Hardness measurements at the end of the crater revealed that at the last stage of penetration the rod material moves sideways for W heavy metal. Metallographic investigations showed strong micro cracking at the crater tip by applying pure W material.

References

- [1] Lach E, Koerber G, Scharf M, Bohmann A. Comparison of nitrogen alloyed austenitic steels and high strength armor steels impacted at high velocity, Hypervelocity Impact Symposium, Huntsville/AL, USA, 16-19 November, 1998.
- [2] Feichtinger HK. Concepts of nitrogen solubility, high nitrogen steels, HNS 93, In: Proceedings 3rd Intern.

Lach, et al. / International Journal of Impact Engineering

- Conference, Kiev, 1993 Ed.: Inst. Met. Physic, Academie of Science Ukraine.
- [3] Stein G, Menzel J, Choudry A. Industrial manufacture of massively nitrogen alloyed steels. In: *Special Melting and Processing Technologies*, San Diego, New Jersey: Noyes Publications, 1988.
 - [4] Uggowitzer PJ. Festigkeit und Zähigkeit austenitischer Stickstoffstähle Habilitationsschrift. ETH, Zürich, 1992.
 - [5] Paulus N. Entwicklung von stickstofflegierten austenitischen Stählen höchster Festigkeit. Diss. ETH, Zürich, Nr.: 10899, Zürich, 1994.
 - [6] Lach E, Werner E, Bohmann A, Scharf M. Deformation behavior of nitrogen alloyed austenitic steels at high strain rates. *Advanced Engineering Materials*, 2000, 2, No. 11.
 - [7] Fréchar S, Redjaimia A, Lach E, Lichtenberger A. mechanical behavior of nitrogen alloyed austenitic stainless steels hardened by warm rolling. *Materials Science and Engineering A*, 2006, pp. 219-224